

Finding the Instability Strip for Accreting Pulsating White Dwarfs from HST and Optical Observations ¹

Paula Szkody², Anjum Mukadam², Boris T. Gänsicke³, Arne Henden⁴, Matthew Templeton⁴, Jon Holtzman⁵, Michael H. Montgomery⁶, Steve B. Howell⁷, Atsuko Nitta⁸, Edward M. Sion⁹, Richard D. Schwartz¹⁰, William Dillon⁴

ABSTRACT

Time-resolved low resolution Hubble Space Telescope ultraviolet spectra together with ground-based optical photometry and spectra are used to constrain the temperatures and pulsation properties of six cataclysmic variables containing pulsating white dwarfs. Combining our temperature determinations for the five pulsating white dwarfs that are several years past outburst with past results on six other systems shows that the instability strip for accreting pulsating white dwarfs ranges from 10,500-15,000K, a wider range than evident for ZZ Ceti pulsators. Analysis of the UV/optical pulsation properties reveals some puzzling aspects. While half the systems show high pulsation amplitudes in the UV compared to their optical counterparts, others show UV/optical amplitude ratios that are less than one or no pulsations at either wavelength region.

Subject headings: cataclysmic variables — stars: individual(PQ And, RE J1255+266, SDSS J074531.92+453829.6, SDSS J091945.11+085710.0, SDSS J133941.11+484727.5, SDSS J151413.72+454911.9) — stars: oscillations — ultraviolet:stars

²Department of Astronomy, University of Washington, Box 351580, Seattle, WA 98195

³Dept. of Physics, University of Warwick, Coventry CV4 7AL, UK

⁴American Association of Variable Star Observers, 25 Birch Street, Cambridge, MA 02138

⁵Department of Astronomy, New Mexico State University, Box 30001, Las Cruces, NM 88003

⁶Department of Astronomy, University of Texas, C1400, Austin, TX 78712

⁷NOAO, 950 N. Cherry Ave., Tucson, AZ 85719

⁸Gemini Observatory, 670 N A'ohoku Pl., Hilo, HI 96720 and Subaru Telescope, 650 N A'ohoku Pl., Hilo, HI 96720

⁹Dept. of Astronomy & Astrophysics, Villanova University, Villanova, PA 19085

¹⁰Galaxy View Observatory, Sequim, WA 98382

1. Introduction

In the decade since the white dwarf in the cataclysmic binary system GW Lib was found to show non-radial pulsations (Warner & van Zyl 1998), a dozen more systems of this type have been discovered (Warner & Woudt 2004; Woudt & Warner 2004; Araujo-Betancor et al. 2005a; Vanlandingham et al. 2005; Patterson et al. 2005a,b; Mukadam et al. 2007; Gänsicke et al. 2006; Nilsson et al. 2006; Patterson et al. 2008; Pavlenko 2009). For convenience, we will refer to the objects found from the Sloan Digital Sky Survey as SDSShhmm±deg i.e. SDSS0745+45. The work on all the known objects has allowed some progress toward understanding how accretion affects the instability zones. While normal non-interacting white dwarfs with hydrogen atmospheres (DAVs or ZZ Ceti stars) show pulsations if they have temperatures in the range of 10,800-12,300K with some dependence of the temperature range on $\log g$ (Koester & Holberg 2001; Bergeron et al. 2004; Gianninas et al. 2006; Mukadam et al. 2006; Castanheira et al. 2007), the white dwarfs in cataclysmic variables (CVs) are known to be heated by accretion (summaries in Sion 1991; 1999; Townsley & Gänsicke 2009). Moreover, CV white dwarfs typically rotate an order of magnitude more rapidly than single DA pulsators, and have solar composition or subsolar metal composition accreted atmospheres. With very few exceptions, the temperatures of non-magnetic white dwarfs in CVs are above 12,000K and so they were previously not expected to be ZZ Ceti type pulsators. However, HST ultraviolet observations of GW Lib clearly showed high amplitude pulsations as well as a high temperature (Szkody et al. 2002a). In addition, the best fit to the data occurred with a 2-temperature model, with 63% of the white dwarf at a temperature of 13,300K and the rest at 17,100K. It was not known if the dual temperature was related to the pulsation or to the presence of a hotter boundary layer where the accretion disk meets the white dwarf.

The existence of the pulsations at such a high temperature led to speculation that the pulsations in GW Lib could be due to a higher mass white dwarf (Townsley, Arras & Bildsten 2004) since a shift in g of about a factor of 10 can shift the blue edge of the H/HeI instability strip to hotter temperatures by about 2000 K. They also stated that the effects of accretion i.e. heavier elements in the atmosphere of the white dwarf, or a faster spin than present in ZZ Ceti pulsators could affect their models. Arras et al. (2006) accomplished a more detailed study that showed that the atmospheric composition of the accreting white dwarf is significant for determining the location of the instability strip. They discovered that

¹Based on observations made with the NASA/ESA Hubble Space Telescope, obtained at the Space Telescope Science Institute, which is operated by the Association of Universities for Research in Astronomy, Inc., under NASA contract NAS 5-26555, and with the Apache Point Observatory 3.5m telescope which is owned and operated by the Astrophysical Research Consortium.

accreting model white dwarfs with a high He abundance (> 0.38) would form an additional hotter instability strip at $\sim 15,000$ K due to HeII ionization.

However, the discovery of pulsations in V455 And (Araujo-Betancor et al. 2005a) and a subsequent snapshot HST spectrum showed that this white dwarf was in the normal ZZ Ceti instability zone (within the uncertainties), with $T_{wd} \sim 10,500$ K and $\log g=8$, thus very different from GW Lib. Arras et al. (2006) suggested that the differences in the two objects could be due to differences in the mass of the white dwarf and to the He abundance in the driving zone. Temperatures determined for three more accreting pulsators provided further confusion (Szkody et al. 2007), as all three systems (SDSS0131-09, SDSS1610-01, SDSS2205+11) showed white dwarfs with temperatures of 14,500-15,000K. Thus, it was not clear if GW Lib or V455 And was the normal case for pulsating white dwarfs in CVs. Further complicating the issue was the fact that the other known cool non-magnetic white dwarf in a CV (EG Cnc) shows no evidence of pulsations even though its temperature is 12,300K (Szkody et al. 2002b) and there are several CVs with T_{eff} near 15,000K as well that don't pulsate e.g. WZ Sge, BC UMa, SW UMa (Sion et al. 1995; Gänsicke et al. 2005). The situation for CVs containing magnetic white dwarfs is similar. Araujo-Betancor et al. (2005b) determined temperatures for seven systems with magnetic white dwarfs and found a range of 10,800-14,200K but none are known to show any signs of pulsations.

Our past HST observations of GW Lib, SDSS0131-09, SDSS1610-01 and SDSS2205+11 showed similar pulsation frequencies in the UV as the optical, with increased amplitudes (6-17) in the UV over the optical. This amplitude ratio is consistent with low order modes (Robinson et al. 1995). Each non-radial pulsation mode can be described with a unique set of indices. Mode identification is essential in asteroseismology to determine the inner structure of the stars. The non-radial luminosity variations observed in white dwarfs are almost entirely due to temperature fluctuations (Robinson, Kepler & Nather 1982). The stellar surface is divided into zones of higher and lower T_{eff} depending on the degree of spherical harmonic ℓ . Since the stellar disk can't be resolved, geometric cancellation results in smaller observable amplitudes for these modes. At UV wavelengths, the increased limb darkening decreases the contribution of zones near the limb, so modes with $\ell=3$ are canceled less effectively in the UV compared to the lower $\ell \leq 2$ modes. But $\ell=4$ modes do not show a significant change in amplitude as a function of wavelength. Robinson et al. (1995) suggested a new mode identification technique based on this effect. While the amplitude ratios for SDSS1610-01 were consistent with those expected for an $\ell=1$ mode and $T_{eff}=12,500$ K white dwarf, the derived temperature from the spectral fit was 14,500K (Szkody et al. 2007). In addition, long term optical coverage of GW Lib (van Zyl et al. 2004) and SDSSJ0131-09 (Szkody et al. 2007) showed that there is a high degree of variability in the amplitudes of the pulses so that at times, some of the periods are not visible. This is normal behavior (termed amplitude

modulation) that is observed in the cool ZZ Ceti stars e.g. Kleinman et al. (1998), Mukadam et al. (2007).

In order to gain further insight into the location of the instability strip for accreting white dwarf pulsators, and to constrain the mode identification of the observed pulsation periods, we obtained HST and nearly simultaneous optical observations of six other CV systems known to contain pulsating white dwarfs (PQ And, REJ1255+26, SDSS1514+45, SDSS1339+48, SDSS0745+45, SDSS0919+08 and SDSS1514+45). The basic properties known for these six objects, along with the full SDSS names, are given in Table 1. Some preliminary results appear in Mukadam et al. (2009).

2. Observations

2.1. HST Ultraviolet Data

The Hubble Space Telescope (HST) Solar Blind Channel (SBC) on the Advanced Camera for Surveys (ACS) was used to observe each of the six objects for 5 satellite orbits with either grating PR110L or PR130L. While both gratings provide spectra from $\sim 1200\text{\AA}$ to $\sim 2000\text{\AA}$, the PR110L extends slightly bluer while the PR130L has increased sensitivity near 1300\AA . In both cases, the prism produces non-linear resolution, with about 2\AA pixel^{-1} (PR110L) and 1\AA pixel^{-1} (PR130L) at 1200\AA and about 40\AA pixel^{-1} at 2000\AA . Since there is no time-tag mode for ACS, 60 or 61s integrations times were used throughout 5 HST orbits on each source. With the setup time during the first orbit, there were 134 or 138 integrations on each object. The dead-time between integrations was 40s so the time resolution is 100 or 101s. The initial exposure and centering of the target was done with the F140LP filter with integration times of 25-60s depending on the brightness of the source. The observation times and gratings are summarized in Table 2.

The HST data were analyzed with the reduction package aXe1.6 provided by STScI. The targets were extracted with different widths that were determined to optimize the spectral and light curve results. For the spectra, a wide extraction (± 17 pixels corresponding to ± 0.5 arcsec) was used to maximize the flux level, whereas a narrower extraction of 5 (PQ And, REJ1255+26), 7 (SDSS0745+45, SDSS1514+45), 11 (SDSS1339+48) and 13 (SDSS0919+08) pixels was used for the light curves to optimize the best S/N for each system. To obtain light curves that could be analyzed for periodicity, all the narrow extractions were summed over the useful wavelength range to obtain one UV flux point per integration time interval.

The entire set of wide-extraction spectra during the five HST orbits were added together

to produce an average final spectrum for each object. These average spectra are shown in Figure 1 ordered by increasing far-UV flux from top to bottom. While the resolution is poor, the emission line of CIV (1550Å) is apparent in all systems. It is clear from this figure that there is a large range in temperature as well as emission line flux for the six objects.

2.2. Optical Data

Due to the remote but possible chance of an outburst during the HST observations that could produce more UV light than the limits of the ACS detector, each system was monitored prior to and during each HST observation by amateurs (from the American Association of Variable Star Observers) and professional astronomers worldwide. These observations showed all six systems to be close to quiescent values. The outburst history of the six objects is given in Table 1. While PQ And and REJ1255+26 had published outbursts in the literature, the previous outburst of SDSS0745+45 was only found from the Catalina Real-time Transient Survey (Drake et al. 2009) which recorded an outburst with a minimum amplitude of 5 mag in 2006 October, with the system brightness declining to its quiescent level over many months².

Time-resolved ground-based observations as close in time as possible to the HST UV observations were also coordinated in order to determine the amplitude and period of optical pulsations that would aid in mode identification. Seven observatories (Table 2) participated in providing observations. The Apache Point Observatory (APO) 3.5m telescope was used with the time-series photometric system Agile which uses a frame-transfer CCD and a BG40 filter to provide broad-band blue light. The McDonald Observatory (MO) 2.1m telescope with their time-series system Argos (Nather & Mukadam 2004) and a BG40 filter was used in a similar fashion. The 1m New Mexico State University (NMSU) telescope with a CCD and BG40 filter and the 1m US Naval Observatory Flagstaff Station (NOFS) telescope with a BG38 filter were also used for several nights. The 0.35m Schmidt-Cassegrain telescope equipped with an unfiltered SBIG CCD also provided data from the Sonoita Research Telescope (SRO) in Arizona. In addition to the observations obtained close in time to the HST times, further data on SDSS0919+08 (APO) and on PQ And (using the WIYN 3.5m telescope equipped with OPTIC and a BG39 filter) were taken a year after the HST observations. All photometric points were made using differential photometry with respect to comparison stars on the frames and light curves were constructed using standard IRAF³ programs for

²click on object link in table at <http://nesssi.cacr.caltech.edu/catalina/20050301/SDSSCV.html>

³IRAF (Image Reduction and Analysis Facility) is distributed by the National Optical Astronomy Ob-

sky-subtracted aperture photometry. To search for periodicities, a discrete Fourier transform up to the Nyquist frequency was computed for each object, after first converting the light curves to a fractional amplitude scale by dividing by the mean and then subtracting one. A summary of the optical observations is also given in Table 2.

3. Spectral Results

Figure 1 shows that there is a large range in continuum flux and shape as well as in the emission line flux of CIV (1550Å) for the six objects. Since the core of Ly α does not reach zero for any of the objects, there is an additional source of continuum light other than the white dwarf, although this contribution is small in most cases. This “second component” has been observed in UV observations of most quiescent dwarf novae, and has been modelled in terms of a hot boundary layer (e.g. Long et al. 1993) or an accretion belt (e.g. Gänsicke & Beuermann 1996; Sion et al. 1996). Long et al. (2009) showed that the WD parameters inferred from a composite fit depend only very mildly on the details of the model assumed for the second component.

The CIV (and to a lesser extent CII at 1335Å, SIV at 1400Å and NV at 1240Å) emission lines probably originate in the disk chromosphere. There may also be some contribution from L α from the disk, although the large upturn at Ly α in Figure 1 for SDSS1514, SDSS1339 and SDSS0919 is likely geocoronal. From our past work on CV systems (e.g. Gänsicke et al. 2005), we have derived a procedure to pull out the temperature of the white dwarf. We account for the disk continuum contribution by adding in a component whose flux raises the continuum in the core of Ly α to the value observed. As our objects were observed during (or close to) dwarf nova quiescence, our current understanding of the theory of dwarf nova outbursts suggests that the accretion disk should be very cool and optically thin. Since we do not know the spectral shape of an optically thin accretion disk, we try three possibilities: a black body, a power law and a constant flux level in F_λ . While these possibilities do not model line features from a disk, the disk contribution is generally small in all cases. Finally, we use simple broad Gaussians at the positions of the known UV lines to fill in their contribution. For each disk contribution type, we match the spectrum with a grid of Hubeny white dwarf models (Hubeny & Lanz 1995). The ACS data do not allow us to infer the surface gravity and we hence fix it at $\log g = 8.0$, as well as the metal abundances at 0.01 times their solar value. Assuming $\log g$ higher (lower) by 0.5 dex would result in best-fit

servatories, which are operated by AURA, Inc., under cooperative agreement with the National Science Foundation.

temperatures lower (higher) by ~ 1000 K, which should be considered as a systematic error of our method.

The results of our fits are listed in Table 3. The final resulting temperature of the white dwarf is indeed almost independent on the assumed spectral shape of the second component, but the exercise provides an estimate of the error of our fits (1000K). If one expects a wildly varying white dwarf mass distribution among these objects (which is not suggested by the observations, e.g. Littlefair et al. 2008), the two uncertainties related to the unknown white dwarf mass and the nature of the second component should be added in quadrature.

For completeness, we also include in the Table the results for the 3 objects observed with the SBC in the past (Szkody et al. 2007) that were re-analyzed with the new aXe1.6 software and refit in the same manner as for our six new observations. An example of the fits for the three spectral shapes of the disk are shown for SDSS1339+48 in Figure 2 while the fitting results using a black-body for the disk contribution are shown for all six of our new objects in Figure 3.

As a check on the white dwarf temperature, the g magnitude for the resulting white dwarf model is also listed and compared to the observed SDSS photometric values in Table 3. All the white dwarf values are fainter than observed, which is reasonable given that the accretion disk will have some contribution to the optical light above that of the white dwarf.

For a further exercise in the total spectral fit, we combined the HST data with the available SDSS spectra for 5 of our objects. REJ1255+26 only has SDSS photometry as a spectrum was not obtained. For this object, the $ugriz$ magnitudes were converted to fluxes. The disk component (using the constant distribution) was then subtracted from the SBC spectrum and the result plotted with the optical spectrum. Figure 4 shows the combined UV and optical data for each system along with the best fit white dwarf temperature models within ~ 2000 K. These plots show the goodness of our temperature fits as well as the amount of the disk contribution to the optical flux (the excess seen in the observed fluxes over the model white dwarf).

4. Light Curves

We computed DFTs of all the HST and available optical light curves, and used linear and non-linear least squares analyses to determine periods, amplitudes, and phases of any coherent variability present in the data. White noise was determined by a light-curve shuffling technique where each time value of fractional intensity was randomly reassigned to another existing time value. This shuffling destroys coherent frequencies but keeps the same time

sampling and white noise as the original data. The DFT of the shuffled light curve provides the noise at each frequency; the mean of the average noise from 10 shufflings is taken as the white noise of the light curve and 3 times this value is quoted in our paper as a detection limit for pulsations. The amplitudes are given in millimodulation amplitudes (mma) where 1 mma is a 0.1% change in intensity. The DFTs for the HST data are shown in Figure 5 along with the window functions. The window function is the DFT of a single frequency noiseless sinusoid sampled exactly the same times as the actual light curve. These functions look quite similar to each other as the HST data for all six systems is sampled in almost the same way (since we deleted data points when the background noise was too high, the sampling is not completely identical for all six targets). A summary of the observed periods and limits from the HST and optical data is contained in Table 4, and the details for each system are discussed below.

4.1. PQ And

For this system, the ground and space observation time overlaps for 4 hrs (Table 2), so periods and amplitudes can be optimally compared. Figures 5 and 6 show the DFTs for the UV and optical data obtained on 2007 Sept. 13. The ground data were obtained with a smaller telescope but the observation interval is longer so that the mean noise is lower (5 mma) than for the UV data (14 mma). While the optical data show the presence of two periods (2337 and 1285s) with amplitudes near 20 mma, there is no significant pulsation evident in the UV. This lack of UV pulsations is surprising and without explanation. The 1285s optical period is the pulsation period reported by Vanlandingham et al. (2005) (Table 1) and the data on 2007 Sept. 15 and 17 show a similar period within the errors. Thus, we regard this as the non-radial pulsation. The 2337s period is not repeated on the other dates and is likely due to flickering noise.

Since the four previous systems observed with HST had shown pulsation amplitudes at least 6 times higher in the UV than the optical, consistent with $\ell=1$ or 2 modes, we would expect a UV amplitude of at least 60 mma at the 1285s period that was evident in the optical within the same time interval. Thus, the lack of detection of any pulsation in the UV implies a high ℓ mode in this system, if the optical periodicity at 1285s is a non-radial pulsation. High ℓ modes ($\ell > 2$) have never been clearly and unambiguously identified in the ZZ Ceti stars. For example, Thompson et al. (2004) identified the 141.9s period in PY Vul (G185-32) as an $\ell=4$ mode, but Pech et al. (2006) suggest that it is an $\ell=2$ mode. Furthermore, they explain that the low value of UV/optical amplitude could be attributed to a resonance between the $\ell=2$ mode and nearby $\ell=3$ and $\ell=5$ modes, which remain undetectable.

The high quality WIYN data obtained a year after the HST observation show an even higher amplitude new periodicity at 679s along with its sub-harmonic at 1355s (Figure 7). Harmonics and linear combinations in our data could arise as a result of non-linearities introduced by relatively thick convection zones (Brickhill 1992, Brassard et al. 1995, Wu 2001, Montgomery 2005). However, since we observe a sub-harmonic at $2P = 1355\text{s}$ and do not detect a harmonic at $P/2 = 339.5\text{s}$, we can rule out convection as the likely cause of the observed non-linearity. Since there is only one observation of this new periodicity, it is possible that both the 679s period and its sub-harmonic at 1355s were caused by flickering. Should frequent monitoring of the system fail to reveal the 679s period again, then the flickering hypothesis is likely. If however the 679s mode proves to be persistent, then it might be an unusual pulsation mode with an observed sub-harmonic instead of a typical harmonic. As a pulsation mode, we could explain its appearance and the absence of previously observed modes as due to amplitude modulation. Amplitude modulation is apparent in GW Lib (Van Zyl et al. 2004) and SDSS0131-09 (Szkody et al. 2007) and also the ZZ Ceti G29-38 (Kleinman et al. 1998). We currently favor the idea that the 679s mode and its sub-harmonic at 1355s are caused by flickering.

4.2. SDSS0745+45

The HST observations of this system took place in the midst of a ground-based run of several nights at McDonald Observatory and SRO. Both observatories overlapped with HST times for about 2.5 hrs (Table 2). While the light curve is highly modulated in both the UV and optical, the modulation is at the long period of 86 min (and its 2nd harmonic at 43 min and 3rd harmonic at 28 min), not within the previously observed range of pulsation periods between 1166-1290s that were clearly evident during 7 nights from 2005 Oct through 2006 Jan (Mukdadam et al. 2007). Figure 8 shows the intensity curves and DFTs for the 2007 data in comparison to that of 2006. While the pulsation is clearly evident in the light curves in 2006, it disappeared at the time of the HST observation. Combining the 4 nights of optical data from 2007 Oct 30-Nov 2, we obtain a 3σ limit to the pulsation amplitude of 8.5 mma. The same limit from the HST data is 12 mma (Figure 5).

Further complicating the issue of the disappearance of the pulsation is the origin of the 86 min modulation. This period (or its harmonics) was evident in 2 of the 7 nights in 2005-2006 where it was presumed to be the orbital period (Mukadam et al. 2007). However, recent spectroscopy (John Taylor 2009, private communication) has revealed an orbital period of 77.8 ± 1.5 min. Combining the 4 nights of photometry listed in Table 4, we obtain periods of 89.3 ± 0.02 min and 43.23 ± 0.01 min. Averaging these numbers (weighted inverseley as the

squares of the uncertainties), we obtain a photometric period of 87.4 ± 1.3 min. Clearly, the spectroscopic period is significantly less than the photometric period. Photometric periods that are 2-4% longer than spectroscopic periods are usually ascribed to superhumps, a phenomenon usually observed following outbursts in short period systems due to precession of an eccentric disk caused by the heating from the outburst (Warner, 1995; Patterson 2001). While it is unusual to have a superhump present at quiescence, one is also apparent in V455 And (Araujo-Betancor et al. 2005a). It is perhaps even more unusual that the periods are so different in SDSS0745+45 (12%). Even if the error bars are underestimated by a factor of 2, the difference between the spectroscopic and photometric periods is still 5%. While this difference is 2.8% in V455 And, there is a one-day alias in the photometric period so the difference could possibly be as large as 9.2%, similar to what we find for SDSS0745+45.

As previously noted, the detection of an outburst around mid-Oct 2006 from the Catalina Sky Survey data means it is likely that the white dwarf in SDSS0745+45 had not completely cooled to its quiescent temperature by the time of the HST observation. Indeed, this object is the hottest one of all the objects we have observed, which is consistent with it having been heated during the outburst. Past work on the cooling times of white dwarfs following outbursts e.g. WZ Sge (Slevinsky et al. 1999; Long et al. 2003; Sion et al. 2003; Godon et al. 2006), and AL Com (Szkody et al. 2003) have shown that this cooling can take more than 3 years. The outburst could have caused some increase in the eccentricity of the disk that causes the long period modulation to be more prominent than pre-outburst. We expect the white dwarf to continue to cool during the next two years and the pulsations to resume, while the long period modulation decreases.

4.3. SDSS0919+08

Whereas five out of six past optical light curves of this object from 2005 Dec to 2007 Mar showed a period near 260s with amplitudes of 7-16 mma (Mukadam et al. 2007), Figure 5 shows that the HST data in 2007 Nov only reveals a harmonic of the orbital period at 40.75 min, with a limit of 15 mma to any shorter term periodicity in the UV (the two peaks on both sides of the 40 min period are aliases). Optical data obtained 2 days prior to the HST observations also reveal no period to a limit of 4 mma (Figure 10) and the data at the end of 2008 show no pulsation to a limit of 7 mma (Table 4). Since there are no known outbursts of this system, and the white dwarf temperature is not high, it is not at all clear why the white dwarf in this system has stopped pulsating. Mukadam et al. (2007) thought the 260s period was a close doublet and the one night it was not observed in their data could be a beating of the two frequencies. However, the lack of periods on the three separated

days of observations in our data and especially the lack of pulsations in the UV indicates this system has actually stopped pulsating. It is possible that if this system is close to the edge of its instability strip, accretion related heating could push it outside. However, the amount of accretion would need to be small enough that it would not noticeably affect the visual magnitude of the system.

4.4. SDSS1339+48

From three nights of photometry in 2005, Gänsicke et al. (2006) identified a prominent pulsation at a period of 641s, as well as a long period at either 320 or 344 min but no modulation at the spectroscopically determined period of 82.52 min. Neither our HST data (Figure 5) nor our ground-based photometry obtained two days prior to the HST data (Figure 10) show the pulsation period of 641s. The HST data do show one significant long period at 7.4 hrs and two short periods (210.3 and 229.6s) that are close to the Nyquist frequency for the data resolution but just below the 3σ noise level of 53 mma. The optical data reveal none of these periods but do show a period consistent with the orbital period (within the error bars), as well as a period at 1539s. Due to the limited data, it is difficult to conclude that any of these periods result from anything other than flickering or accretion effects. However, it is clear that there is no large amplitude UV pulsation at the previously determined optical period of 641s .

4.5. SDSS1514+45

Our optical data from APO (Figure 11) have about 1.5 hrs of overlap with the HST UV data for this source. Neither wavelength shows the 559s period previously reported by Nilsson et al. (2006). As that period has not been evident since their data in 2005, further observations are needed to confirm if this really is a pulsator with a changing amplitude.

The DFT from the UV data (Figure 5) does show a longer period at 88.8 min which could be the orbital period. The faintness of this system has precluded the determination of an orbital period from spectroscopy at the current time. There is a period near 700s that is almost at the 3σ limit, but as this is not evident in the optical, it is likely related to flickering.

4.6. REJ1255+26

Our APO optical time-resolved data on this system only encompass one light curve on the night following the HST observations. The UV data show the 1.9 hr orbital period but a limit of 52 mma to any shorter periods. The optical data (Figure 13) reveals two short periods at 654.5 and 582.1. Patterson et al. (2005b) had previously found a period of 668s. As in PQ And, the presence of optical periods without detection in the UV at a higher amplitude implies a high ℓ mode of pulsation, if the periods are due to non-radial pulsations.

5. Discussion

Figures 1,3,4 and Table 3 show that the 9 systems with similar SBC data show a range of temperatures from 10,000-17,000K. The hottest temperature white dwarf exists in SDSS0745+45. However, since that system underwent an outburst only 1 year prior to the HST observation, it is likely that its white dwarf has not cooled to its quiescent value. This is corroborated by the lack of pulsations evident in the HST data. Long term studies of the white dwarf cooling in low accretion rate CVs with short orbital periods have shown that it takes more than 3 yrs for the white dwarf to cool following outburst (Piro et al. 2005; Godon et al. 2006). Eliminating SDSS0745+45 and adding in the temperatures derived from STIS observations of GW Lib (15,400 for a black body disk contribution; Szkody et al. 2002a) and V455 And (11,500; Araujo-Betancor et al. 2005a), and from the eclipse modeling of SDSS1507+52 (11,000; Littlefair et al. 2008), gives an instability range of 10,000-15,000K with the CV pulsators spread throughout this range. Thus, if the higher temperatures of pulsating accretors relative to ZZ Ceti stars is due to mass or composition, then no unique parameter characterizes the accreting pulsators. Half of the 11 temperatures lie within the ZZ Cet instability strip (within the error bars and with a $\log g$ of 8) and half are hotter. Figure 13 shows our 11 quiescent temperatures along with the ZZ Ceti empirical instability strip (Gianninas et al. 2007). While a few of the systems could fall within the strip if they have massive white dwarfs (higher $\log g$), it would be difficult to have mass be the primary cause of the width of the strip. Arras et al. (2006) can account for increased width with an increase in He in the driving zone.

Besides the width of the instability strip for accreting pulsators, the other oddity is why all CVs with white dwarfs in the temperature range of the known pulsators do not show pulsations. Table 6 lists all the white dwarfs with reliable temperature determinations (from the recent summary in Townsley & Gänsicke 2009, with the addition of SDSS1507+52 from Littlefair et al. 2008) and they are also plotted in Figure 13. The two closest systems to the ZZ Cet instability strip are EG Cnc (at the blue edge) and SDSS1035+05 (at the red edge).

Further monitoring of these systems is needed to determine if they never pulsate or if they were observed during a hiatus of their pulsations.

GW Lib still stands out as the only system among the 11 with available UV spectra in which the best fit is obtained with a dual temperature white dwarf rather than a white dwarf plus an accretion disk. It is the only system in which the core of Ly α does reach zero. If this dual temperature is due to a boundary layer ring that is hotter due to the accretion, it is not clear why this is not the case in the other 10 systems, especially for SDSS0745+45 which is heated by the recent outburst.

Within the limited numbers, there does not seem to be any correlation of white dwarf temperature with orbital period as would be expected if the white dwarfs are cooling due to decreasing mass accretion rate as they evolve to shorter orbital periods (Howell, Nelson & Rappaport 2001). Figures 2-4 give some indication of the accretion luminosity (hence white dwarf mass and accretion rate) from the contribution of the accretion disk to the light. Excluding SDSS0745+45, whose white dwarf is likely not at its quiescent temperature, the white dwarfs in our models contribute 75-89% of the UV light and 42-75% of the optical light for the other 8 objects in Table 3. The three hottest white dwarfs (SDSS2205+11, SDSS0131-09 and SDSS1610-01) do have the three highest disk contributions to the optical light (50, 58 and 41%) which is consistent with a higher mass white dwarf or a higher accretion rate that would heat the white dwarf.

Figure 14 shows the accreting pulsators as well as the non-pulsating white dwarfs (Table 6) as a function of their orbital period. As noted in Gänsicke et al. (2009b), most of the pulsating white dwarfs lie in a period regime termed the "period spike" between 80-86 min. The most egregious outlier is REJ1255+266 near 2 hrs. Since the period determination for REJ1255+266 is a photometric one and we now know that at least 2 of our pulsating accretors (V455 And and SDSS0745+45) show different photometric periods than spectroscopic, this period may be suspect and awaits a spectroscopic determination. However, the pulsator SDSS1507+52 has a period of 66.6 min determined from eclipses (Patterson et al. 2008) so it appears this one really is an outlier to the rest of the group. GW Lib and SDSS0745+45 (not shown on the plot as its temperature may not be its quiescent one) are outside the spike as well. It is clear from Figure 14 that most of the accreting pulsators are concentrated in a narrow period range near 82 min. It is easy to explain why longer period systems are not evident as pulsators, as those typically have increased mass accretion rates which can hide the white dwarf, and thus make pulsations harder to detect. But it is not obvious why the pulsations would not be present in systems with shorter orbital periods and why the transition is so abrupt.

A pure instability strip with non-pulsators outside and only pulsators within, implies

that pulsations are an evolutionary phase along the cooling track (Fontaine et al. 1982, 2003, Bergeron et al. 2004, Castanheira et al 2007). In other words, *all* accreting white dwarfs would undergo the pulsation phase. An impure instability strip with pulsators and non-pulsators mixed in implies that parameters other than the white dwarf temperature and mass are at play in deciding whether the star will pulsate or not (Kepler & Nelan 1993, Mukadam et al. 2004). Our preliminary results indicate an impure strip with 13 non-pulsators in the range of 10500–15400 K; this lends credence to the theory that He abundance is the third parameter that decides the shape of the instability strip for accretors (Arras et al. 2006).

In addition to the temperature data, we now also have ten systems with pulsation properties determined from UV through optical wavelengths (Table 5). This table shows a perplexing mix of results. While several objects (GW Lib, SDSS0131-09, SDSS1610-01 and SDSS2205+11) behave similarly to ZZ Ceti stars in having high UV/optical amplitude ratios, and similar periods evident in UV and optical, others (PQ And and REJ1255+26) have very low UV/optical amplitude ratios or show no pulsations in either UV nor optical at the time of our observations (SDSS0745+45, SDSS0919+08, SDSS1339+48, SDSS1514+45). The absence of pulsations in SDSS0745+45 can be explained by its recent outburst, which has likely heated its white dwarf and moved it out of the instability strip. This explanation is corroborated by the lack of optical and UV pulsations of GW Lib following its recent outburst (Szkody et al. 2009; Copperwheat et al. 2009). SDSS1514+45 suffers from insufficient data to confirm pulsations. However, there is no clear explanation for SDSS0919+08 and SDSS1339+48. Recent observations of SDSS2205+11 (Southworth et al. 2008) also show a lack of pulsation on two nights as compared to previous years (Warner & Woudt 2004; Szkody et al. 2007). While SDSS1339+48 is just outside the blue edge of the ZZ Cet instability strip for $\log g=8$ (Figure 13), which might account for its lack of pulsation if its white dwarf underwent a slight temperature increase, SDSS0919+08 and SDSS2205+11 are much further away from this edge. Southworth et al. (2008) discuss several possible reasons for the lack of pulsations (destructive interference, changes in the thermal state of the driving region, or changing visibility of the modes over the surface of the white dwarf) but conclude further observations over long timescales are needed to sort out the cause. While different frequencies are known to be dominant at different times during the course of several years in GW Lib (van Zyl et al. 2004) and in SDSS0131-09 (Szkody et al. 2007), information as to the length of time that systems show no pulsations at all is not available.

6. Conclusions

Our recent ultraviolet and optical data on six systems combined with past data on six others produces a dataset of 12 accreting pulsating white dwarfs with temperatures (Tables 3, 6) and ten with pulsation properties determined from UV through optical wavelengths (Table 5). These datasets are beginning to contain enough objects to begin to see some trends as well as to reveal some abnormalities.

- The temperature range for the 11 objects that have been in quiescence for years are in the range of 10,500-15,000K. This range includes the temperatures found in ZZ Ceti pulsators but extends to higher temperatures. The temperatures appear to uniformly spread throughout the entire range, but we are still in the domain of small number statistics. Since we do not have masses or He abundances for these 11 systems, it is difficult to test the predictions of (Arras et al. 2006) as to the cause of the width of the strip.
- Several CVs are known to have white dwarfs with temperature within this range of 10,500-15,000K but they are not pulsating. Table 6 presents a list of the white dwarfs in disk-accreting CV that have reliable quiescent temperatures (from Townsley & Gänsicke 2009, Littlefair et al. 2008, and this work) and whether they have shown pulsations. It is unclear why not all CVs in this temperature range are pulsating. In addition to the disk-accretors, there are an additional 11 highly magnetic white dwarfs in CVs (Polars) in the Townsley & Gänsicke (2009) list within this temperature range, none of which show pulsations.
- GW Lib is the only system among the 11 with UV spectra in which the best fit is obtained with a dual temperature white dwarf rather than a white dwarf plus a disk contribution.
- The object that is one year past outburst (SDSS0745+45) has a hotter temperature (17,000K) and is no longer pulsating. This corroborates past work that shows the white dwarfs in CVs are heated for several years following outburst (Piro et al. 2005; Godon et al. 2006) and it is likely that this object has moved out of the instability strip.
- Four systems (GW Lib, SDSS0131-09, SDSS1610-01 and SDSS2205+11) show identical pulsation periods in the UV and optical with high amplitude ratios of UV/opt. These four are similar to the low order modes evident in ZZ Ceti stars; however, the temperatures of all 4 are 14,000-15,000, far outside the range for ZZ Ceti objects.

- Two objects (PQ And and REJ1255+26) have UV/optical amplitude ratios that are less than 1. Both of these objects have white dwarf temperatures of 12,000K, just inside the blue edge of the ZZ Ceti instability strip (Figure 13). If the optical periods observed are non-radial pulsations, this implies a high ℓ mode not unambiguously observed in ZZ Ceti pulsators. It remains a problem for theorists to determine if the differences between accreting and non-accreting white dwarfs could cause this effect.
- Four objects (SDSS0745+45, SDSS0919+08, SDSS1339+48 and SDSS1514+45) did not show pulsations in either UV nor optical. The lack of pulsations in SDSS0745+45 can be explained by its outburst only 1 year prior to the HST data, while SDSS1514+45 has had only minimal observational data in the past (Nilsson et al. 2006), so further data are needed to confirm it as an accreting pulsator. For the other 2 systems, there is no clear explanation for why the pulsations that were evident from several nights of ground-based data in the past have disappeared. Both of these objects are in the intermediate temperature zone (12,500-13,500K) between the normal ZZ Ceti instability edge and the hotter temperatures of the 4 pulsators that do show UV pulsations of high amplitude. Since the temperatures are not high (as in SDSS0745+45), it is unlikely that an outburst has occurred in these 2 systems. It is possible that these pulsators were close to the edge of the instability strip (SDSS0919+08 would have to be high mass to be near the edge), and changes in accretion heating take them in and out of the instability zone. We intend to keep observing these objects to determine if pulsations return at the previous periods.
- Two objects (V455 And and SDSS0745+45) show photometric periods that are longer than the spectroscopic periods by 3-12%. The presence of such periods are typically due to superhumps caused by precessing, eccentric disks in short orbital period CVs during an outburst. If this is the cause in these two objects, it is unusual to find the superhumps during quiescence and even more unusual to have such a large percentage difference in the periods.

To make progress toward understanding the edges of the instability strip and the pulsation modes that relate to the appearance/disappearance of periods at different times, further data are needed. Mass determinations of a few of the hot vs cool white dwarfs can determine how this parameter effects the width of the strip. Continued observations of the systems that have undergone outbursts in 2006-2007 (SDSS0745+45, GW Lib, V455 And and SDSS0804+51) as they re-enter the instability strip following the heating during the outburst will provide valuable information about the modes and depth of heating. Long observation sequences for the objects in Table 6 that are not known to pulsate are needed to place stringent limits on the amplitudes of possible pulsations. The identification of further

accreting pulsating systems will help to enlarge the database on which to draw conclusions about the stability of periods and the behavior as a function of the temperature of the white dwarf.

We gratefully acknowledge the many amateur and professional observers who monitored our objects prior to and during the HST observations which allowed the UV observations to proceed with the knowledge that the objects were at quiescence. Special thanks go to Agatha Raup, Joanne Hughes and Gary Walker. This research was supported by NASA grant HST-GO-11163.01-A from the Space Telescope Science Institute which is operated by the Association of Universities for Research in Astronomy, Inc., for NASA, under contract NAS 5-26555. BTG was supported by a PPARC Advanced Fellowship.

REFERENCES

- Araujo-Betancor, S. et al. 2005a, *A&A*, 430, 629
- Araujo-Betancor, S. et al. 2005b, *ApJ*, 622, 589
- Arras, P., Townsley, D. M. & Bildsten, L. 2006, *ApJ*, 643, L119
- Bergeron, P., Fontaine, G., Billeres, M., Boudreault, S. & Green, E. M. 2004, *ApJ*, 600, 404
- Brassard, P., Fontaine, G., & Wesemael, F. 1995, *ApJS*, 96, 545
- Brickhill, A. J., 1992, *MNRAS*, 259, 529
- Castanheira, B. G. et al. 2007, *A&A*, 462, 989
- Copperwheat, C. M. et al. 2009, *MNRAS*, 393, 157
- Drake, A. J. et al. 2009, *ApJ*, 696, 870
- Fontaine, G., Lacombe, P., McGraw, J. T., Dearborn, D. S. P. & Gustafson, J. 1982, *ApJ*, 258, 651
- Fontaine, G., Bergeron, P., Billeres, M. & Charpinet, S. 2003, *ApJ*, 591, 1284
- Gänsicke, B. T. & Beuermann, 1996, *A&A*, 309, L47
- Gänsicke, B. T., Szkody, P., Howell, S. B. & Sion, E. M. 2005, *ApJ*, 629, 451
- Gänsicke, B. T., et al. 2006, *MNRAS*, 365, 969
- Gänsicke, B. T. et al. 2009, *MNRAS*, in press.
- Gianninas, A., Bergeron, P. & Fontaine, G. 2006 *ApJ*, 132, 831
- Gianninas, A., Bergeron, P. & Fontaine, G. 2007, *ASP Conf. Ser.* 372, 577

- Godon, P., Sion, E. M., Cheng, F., Long, K. S., Gänsicke, B. T. & Szkody, P. 2006, *ApJ*, 642, 1018
- Howell, S.B., Nelson, L. A. & Rappaport, S. 2001, *ApJ*, 550, 897
- Hubeny, I. & Lanz, T. 1995, *ApJ*, 439, 875
- Kepler, S. O. & Nelan, E. P., 1993, *ApJ*, 612, 1052
- Koester, D. & Holberg, J. B. 2001, *ASP Conf. Ser.* 226: 12th European Workshop on White Dwarfs, 226, 299
- Kleinman, S. J. et al. 1998, *ApJ*, 495, 424
- Littlefair, S. et al. 2008, *MNRAS*, 388, 1582
- Long, K. S. et al. 1993, *ApJ*, 405, 327
- Long, K. S. et al. 2003, *ApJ*, 591, 1172
- Long, K. S. et al. 2009, *ApJ*, 697, 1512
- Montgomery, M. H. 2005, *ApJ*, 633, 1142
- Mukadam, A. S. et al. 2004, *ApJ*, 612, 1052
- Mukadam, A. S., Montgomery, M. H., Winget, D. E., Kepler, F. O. & Clemens, J. C. 2006, *ApJ*, 640, 956
- Mukadam, A. S. et al. 2007, *ApJ*, 667, 433
- Mukadam, A. S., Szkody, P., Gänsicke, B. T. & Nitta, A. 2009, *J. Phys. Conf. Ser.* 172, 012069
- Nather, R. E. & Mukadam, A. S., 2004, *ApJ*, 605, 846
- Nilsson, R., Uthas, H., Ytre-Eide, M., Solheim, J.-E. & Warner, B. 2006, *MNRAS*, 370, L56
- Patterson, J. 2001, *PASP*, 113, 736
- Patterson, J., Thorstensen, J. R., Armstrong, E., Henden, A. A., & Hynes, R. I. 2005a, *PASP*, 117, 922
- Patterson, J., Thorstensen, J. R. & Kemp, J. 2005b, *PASP*, 831, 427
- Patterson, J. et al. 2008, *PASP*, 120, 510
- Pavlenko, E. 2009, *J. Phys. Conf. Ser.* 172, 012071
- Pech, D. & Vauclair, G. 2006, *A&A*, 453, 219
- Piro, A. L., Arras, P. & Bildsten, L. *ApJ*, 628, 401
- Robinson, E. L., Kepler, S. O. & Nather, R. E. 1982, *ApJ*, 259, 219

- Robinson, E. L., et al. 1995, *ApJ*, 438, 908
- Schwarz, G. J. et al. 2004, *PASP*, 116, 1111
- Sion, E. M. 1991, *AJ*, 102, 295
- Sion, E. M. et al. 1995, *ApJ*, 439, 957
- Sion, E. M. et al. 1996, *ApJ*, 471, L41
- Sion, E. M. 1999, *PASP*, 111, 532
- Sion, E. M. et al. 2003, *ApJ*, 592, 1137
- Slevinsky, R. J., Stys, D., West, S., Sion, E. M. & Cheng, F. H. 1999, *PASP*, 111, 1292
- Southworth, J., Townsley, D. M. & Gänsicke, B. T. 2008, *MNRAS*, 388, 709
- Szkody, P., Gänsicke, B. T., Howell, S. B. & Sion, E. M. 2002a, *ApJ*, 575, L79
- Szkody, P., Gänsicke, B. T., Sion, E. M. & Howell, S. B. 2002b, *ApJ*, 574, 950
- Szkody, P. et al. 2003, *ApJ*, 126, 1451
- Szkody, P. et al. 2007, *ApJ*, 658, 1188
- Szkody, P. et al. 2009, *ASP Conf. Ser.* 404, 229
- Thompson, S. E., Clemens, J. C., van Kerkwijk, M. H. O’Brien, M. S., & Koester, D. 2004, *ApJ*, 610, 1001
- Townsley, D. M., Arras, P. & Bildsten, L. 2004, *ApJ*, 608, L105
- Townsley, D. M. & Gänsicke, B. T. 2009, *ApJ*, 693, 1007
- Vanlandingham, K. M., Schwarz, G. J. & Howell, S. B. 2005, *PASP*, 117, 928
- van Zyl, L. et al. 2004, *MNRAS*, 350, 307
- Warner, B. 1995, in *Cataclysmic Variable Stars*, CUP
- Warner, B. & van Zyl, L. 1998, *IAU Symp.* 185, 321
- Warner, B. & Woudt, P. 2004, *ASP Conf. Ser.* 310, 382
- Wu, Y. 2001, *MNRAS*, 323, 248
- Woudt, P. & Warner, B. 2004, *MNRAS*, 348, 599

Table 1. Objects Observed with HST

Name	Mag	P_{orb} (min)	Opt Pulse P (sec)	Amp (mma)	Outbursts (yr)	Ref ^a
PQ And	19.1(V)	80.6	1263, 1286	25	1938, 1967, 1988	1,2,3
SDSS0745 ^b	19.0(g)	77.8	1166-1290	45-70	2006	4
SDSS0919	18.2(g)	81.3	260	7-16	none	4
SDSS1339	17.7(g)	82.5	641	25	none	5
SDSS1514	19.7(g)	...	559	12	none	6
REJ1255 ^b	19.1(g)	119.5	668, 1236, 1344	7-30	1994	7

^a1 Schwarz et al. (2004), 2 Patterson et al. (2005a), 3 Vanlandingham et al. (2005), 4 Mukadam et al. (2007), 5 Gänsicke et al. (2006), 6 Nilsson et al. (2006), 7 Patterson et al. (2005b)

^bFull names of objects are: SDSS J074531.92+453829.6; SDSS J091945.11+085710.0; SDSS J133941.11+484727.5; SDSS J151413.72+454911.9; RE J1255+266

Table 2. Summary of Observations

Name	Obs	Instr	Filter	Int(s)	UT Time
PQ And	HST	SBC	PR110L	60x138	2007 Sep 13 03:36-10:45
PQ And	NOFS	CCD	none	180	2007 Sep 13 06:43-12:18
PQ And	NMSU	CCD	BG38	180	2007 Sep 13 05:05-05:51
PQ And	NMSU	CCD	BG38	180	2007 Sep 15 04:33-09:41
PQ And	NMSU	CCD	BG38	180	2007 Sep 19 06:59-11:04
PQ And	WIYN	OPTIC	BG39	25	2008 Oct 21 08:14-10:57
SDSS0745	HST	SBC	PR110L	61x138	2007 Nov 01 02:48-09:57
SDSS0745	MO	Argos	BG40	30	2007 Oct 30 07:13-12:31
SDSS0745	MO	Argos	BG40	30	2007 Oct 31 07:05-12:33
SDSS0745	MO	Argos	BG40	30	2007 Nov 01 07:21-12:26
SDSS0745	MO	Argos	BG40	30	2007 Nov 02 07:17-12:34
SDSS0745	SRO	CCD	none	1200	2007 Oct 31 07:32-12:25
SDSS0745	SRO	CCD	none	900	2007 Nov 01 07:27-12:27
SDSS0919	HST	SBC	PR130L	61x134	2007 Nov 14/15 18:36-01:41
SDSS0919	MO	Argos	BG40	15	2007 Nov 12 10:13-12:43
SDSS0919	NMSU	CCD	BG39	180	2007 Nov 8-15 2 per night
SDSS0919	SRO	CCD	none	300	2007 Nov 14 08:55-12:37
SDSS0919	SRO	CCD	none	300	2007 Nov 15 09:05-10:18
SDSS0919	APO	Agile	BG40	20	2008 Dec 30 10:10-13:28
SDSS1339	HST	SBC	PR130L	61x138	2008 Jan 25 07:42-14:51
SDSS1339	APO	Agile	BG40	15	2008 Jan 23 11:26-12:57
SDSS1514	HST	SBC	PR130L	60x138	2008 May 08 05:24-12:29
SDSS1514	APO	Agile	BG40	40	2008 May 08 03:00-07:00
SDSS1514	APO	Agile	BG40	40,80	2008 May 09 04:53-07:04
REJ1255	HST	SBC	PR110L	61x134	2008 May 14 01:50-08:58
REJ1255	APO	Agile	BG40	40	2008 May 15 03:00-07:02

Table 3. Model Fits to SBC Spectra

Obj+Model	T_{wd} (K)	d(pc)	T_{BB}/PL^a	g_{wd}
SDSS1514+const	10,500	408	...	20.0
SDSS1514+BB	10,000	358	9500	19.9
SDSS1514+PL	10,500	416	1.0	20.1
PQ And+const	12,000	340	...	19.3
PQ And+BB	12,000	361	16,500	19.4
PQ And+PL	12,000	337	-0.16	19.2
REJ1255+const	12,000	403	...	19.6
REJ1255+BB	12,000	543	11,500	20.3
REJ1255+PL	12,000	420	0.90	19.7
SDSS1339+const	12,500	191	...	17.9
SDSS1339+BB	12,500	187	25,000	17.9
SDSS1339+PL	12,500	187	0.08	17.9
SDSS0919+const	13,500	319	...	18.9
SDSS0919+BB	13,500	333	15,500	19.0
SDSS0919+PL	13,500	330	1.0	19.0
SDSS0131+const	14,000	388	...	19.3
SDSS0131+BB	14,500	432	14,000	19.4
SDSS0131+PL	14,000	371	0.66	19.2
SDSS1610+const	14,000	504	...	19.8
SDSS1610+BB	14,500	611	13,500	20.2
SDSS1610+PL	14,500	562	1.0	20.0
SDSS2205+const	14,000	859	...	21.0
SDSS2205+BB	15,000	919	11,000	21.0
SDSS2205+PL	14,000	862	0.66	21.0
SDSS0745+const ^b	17,000	445	...	19.2
SDSS0745+BB	17,000	474	19,000	19.3
SDSS0745+PL	17,000	463	-0.02	19.3

^a T_{BB} is the black body temperature of the 2nd component and PL is the slope of the power law for the 2nd component.

^bAs this object underwent an outburst one year prior to the HST observation, the white dwarf is likely not yet at its quiescent temperature.

Table 4. Summary of Observed Periods and 3σ Limits

Object	Wavelength (\AA)	Period	Amp (mma)	UT Date
PQ And	1200-1820	...	<42	09-13-07
PQ And	optical	$1285\pm 10\text{s}$, $2337\pm 10\text{s}$	22, 22	09-13-07
PQ And	optical	$1309\pm 13\text{s}$	28	09-15-07
PQ And	optical	$1301\pm 13\text{s}$	27	09-19-07
PQ And	optical	$679.0\pm 1.4\text{s}$, $1355\pm 16\text{s}$	28, 10	10-21-08
SDSS0745	1240-1910	...	<12	11-01-07
SDSS0745	optical	$84.4\pm 0.4\text{min}^{\text{a}}$, $44.1\pm 0.3\text{min}^{\text{b}}$	68, 30	10-30-07
SDSS0745	optical	$86.4\pm 0.4\text{min}^{\text{a}}$, $41.5\pm 0.2\text{min}^{\text{b}}$, 27.8 ± 0.2	68, 36, 17	10-31-07
SDSS0745	optical	$91.1\pm 0.8\text{min}^{\text{a}}$	70	11-01-07
SDSS0745	optical	$83.6\pm 0.3\text{min}^{\text{a}}$, $42.2\pm 0.3\text{min}^{\text{b}}$, $28.5\pm 0.2\text{min}$	62, 22, 17	11-02-07
SDSS0919	1226-1955	$40.72\pm 0.09\text{min}^{\text{b}}$	85	11-14/15-07
SDSS0919	optical	...	<4	11-12-07
SDSS0919	optical	...	<7	12-30-08
SDSS1339	1245-1955	$7.39\pm 0.25\text{hr}$	104	01-25-08
SDSS1339	optical	$83.2\pm 3.0\text{min}^{\text{a}}$, $1539\pm 32\text{s}$	24, 14	01-23-08
SDSS1514	1324-1935	$88.8\pm \text{min}^{\text{c}}$	108	05-08-08
SDSS1514	optical	...	<6	05-07-08
REJ1255	1335-1885	$1.91\pm 0.04\text{hr}^{\text{a}}$	76	05-14-08
REJ1255	optical	$54.5\pm 1.0\text{min}$, $582.1\pm 1.7\text{s}$, $654.5\pm 1.9\text{s}$	12, 13	05-15-08

^aOrbital period or superhump period.

^bFirst harmonic of orbital or superhump period.

^clikely orbital period.

Table 5. Summary of UV and Optical Periods and Amplitude Ratios

Object	UV Periods (s)	Opt Periods (s)	UV/opt amplitude
GW Lib	648, 376, 236	646, 376, 237	6-17
SDSS0131	213	211	6
SDSS1610	608, 304, 221	608, 304, 221	6
SDSS2205	576	575	6
PQ And	...	1285	< 1
REJ1255	...	582, 655	< 1
SDSS0745
SDSS0919
SDSS1339
SDSS1514

Table 6. All WDs in Disk CVs with Temperatures of 10,000-15,000K

Name	P_{orb} (hr)	T_{eff} K	Pulsating
SDSS1507+52	1.11	11,000±500	Y
GW Lib	1.28	13,300+17,100	Y
BW Scl	1.30	14,800±900	N
LL And	1.32	14,300±1000	N
PQ And	1.34	12,000±1000	Y
SDSS1610-01	1.34	14,500±1500	Y
V455 And	1.35	10,500±750	Y
AL Com	1.36	16,300±1000	N
SDSS0919+08	1.36	13,500±1000	Y
WZ Sge	1.36	14,900±250	N
SW UMa	1.36	13,900±900	N
SDSS1035+05	1.37	10,500±1000	N
HV Vir	1.37	13,300±800	N
SDSS1339+48	1.38	12,500±1000	Y
SDSS2205+11	1.38	15,000±1000	Y
WX Cet	1.40	13,500	N
EG Cnc	1.41	12,300±700	N
XZ Eri	1.47	15,000±1500	N
SDSS1514+45	1.48?	10,000±1000	Y?
VY Aqr	1.51	14,500	N
OY Car	1.52	15,000±2000	N
SDSS0131-09	1.63	14,500±1000	Y
HT Cas	1.77	14,000±1000	N
REJ1255+26	1.99	12,000±1000	Y
EF Peg	2.00	16,600±1000	N

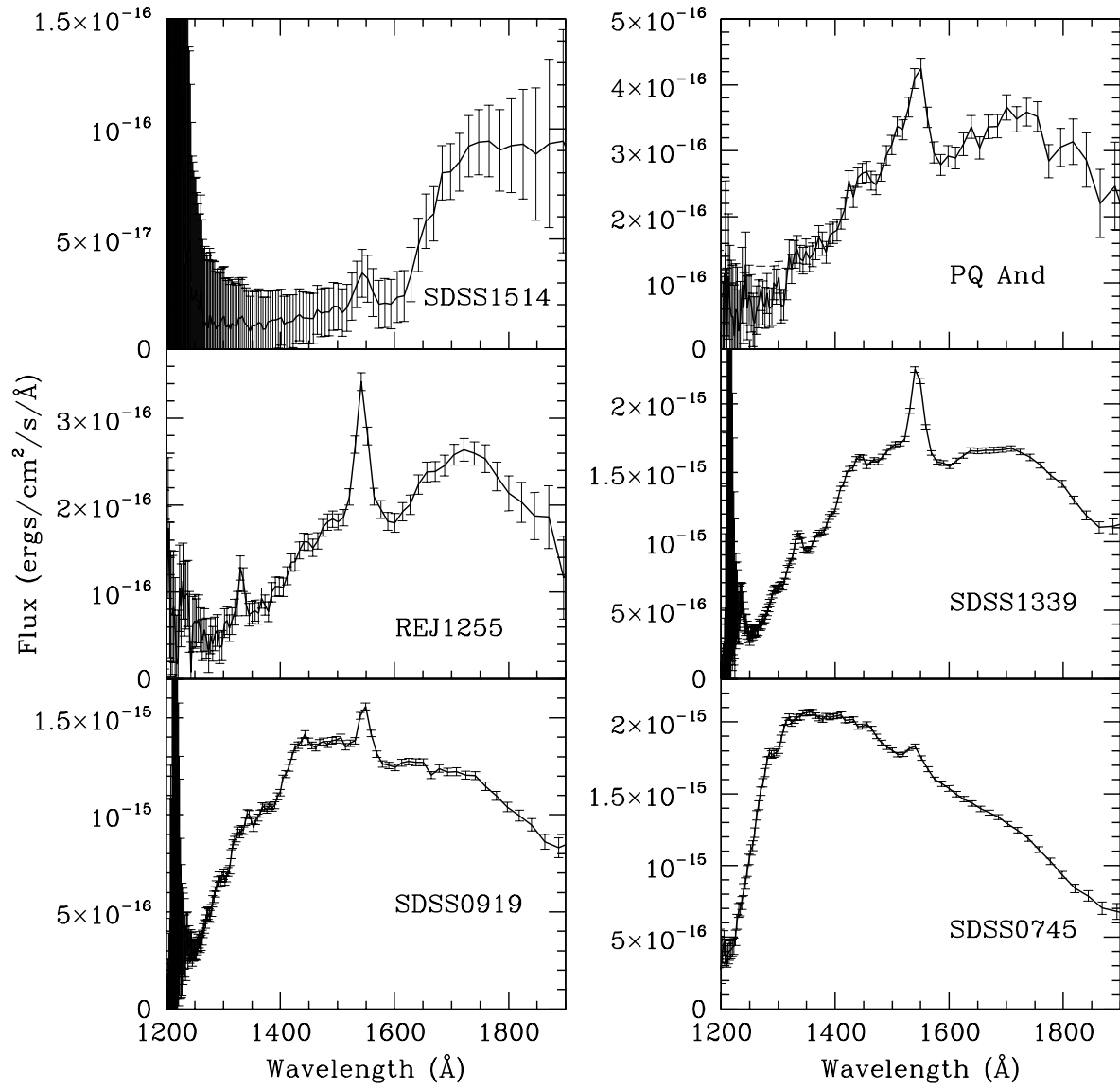


Fig. 1.— HST SBC average spectra of all 6 of our objects using a 17 pixel extraction.

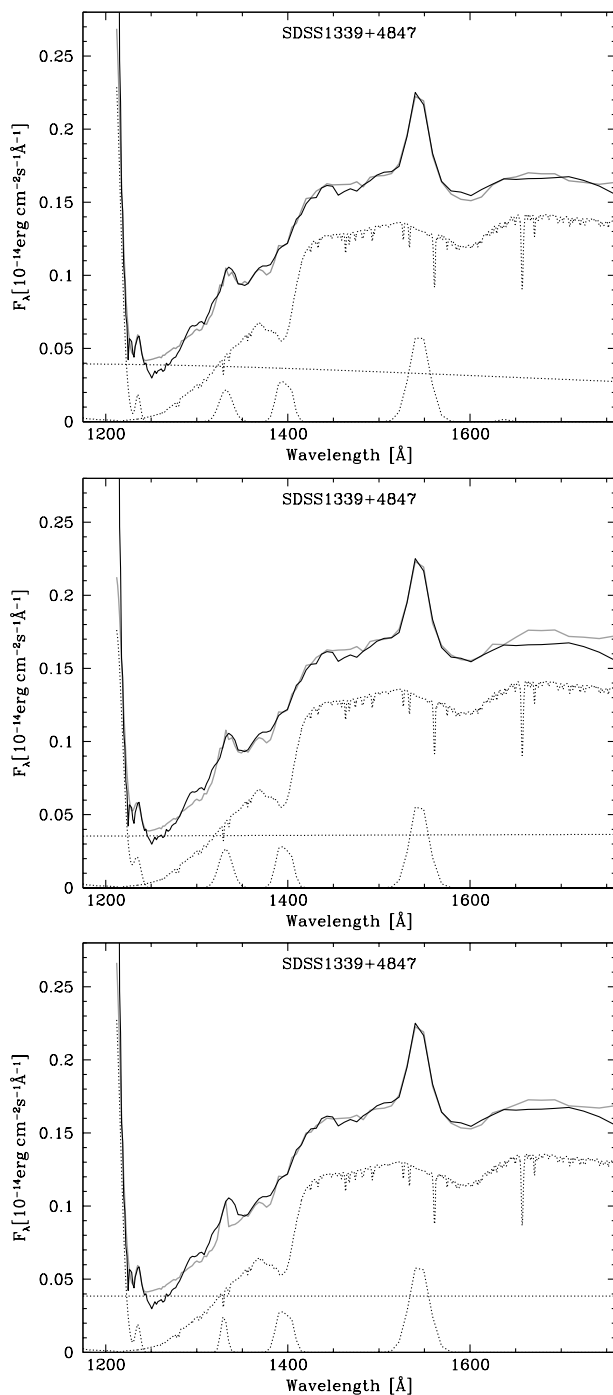


Fig. 2.— White dwarf model (mid curve with absorption lines) fit to the SBC data (dark curve) on SDSS1339+48 with the disk contribution component (lowest lines) of a black body (top), a power law (mid) and a constant (bottom). In each case, the emission lines are approximated by broad Gaussians and the sum of the WD, disk and emission lines is the dotted curve on top of the observed values.

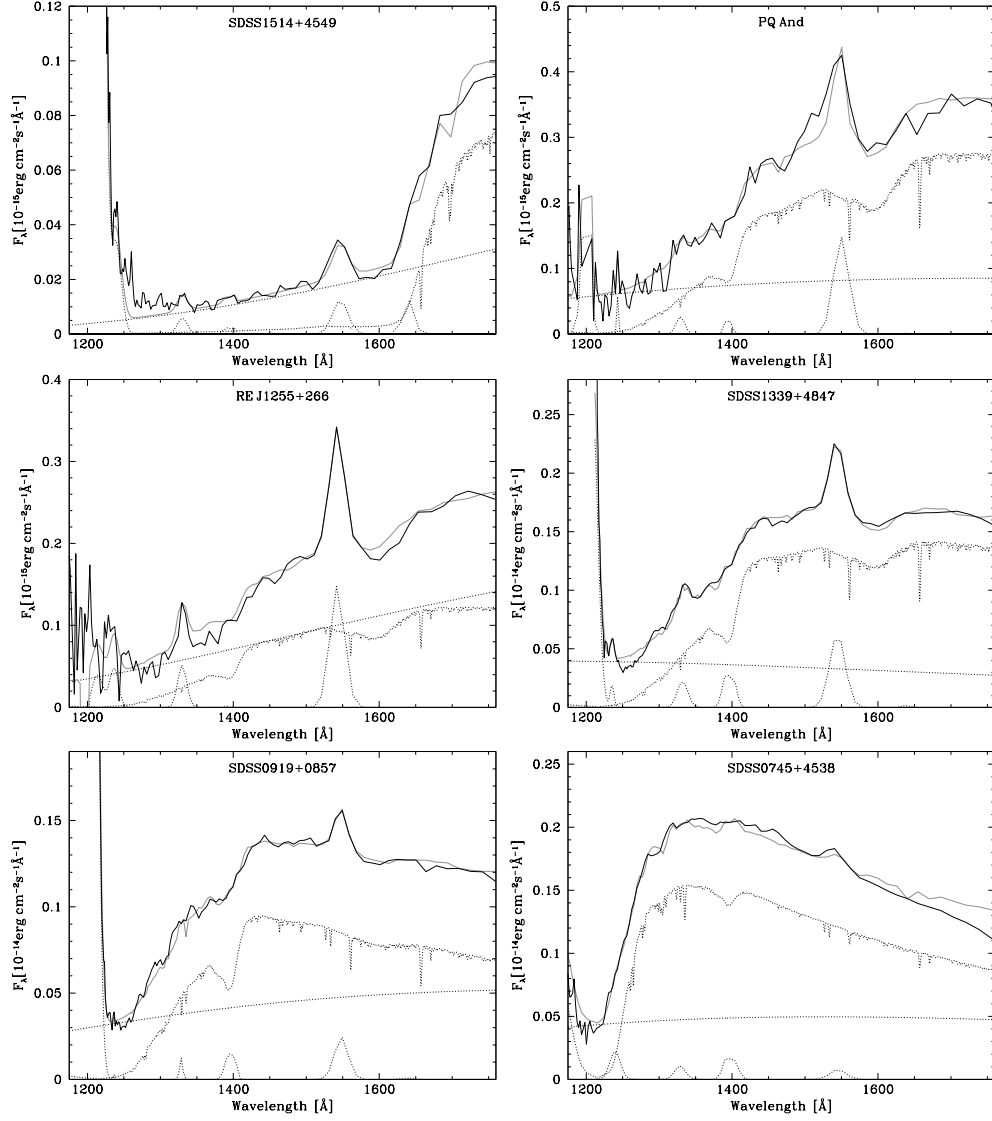


Fig. 3.— White dwarf plus black-body + Gaussian lines model fits to the SBC data for our 6 objects.

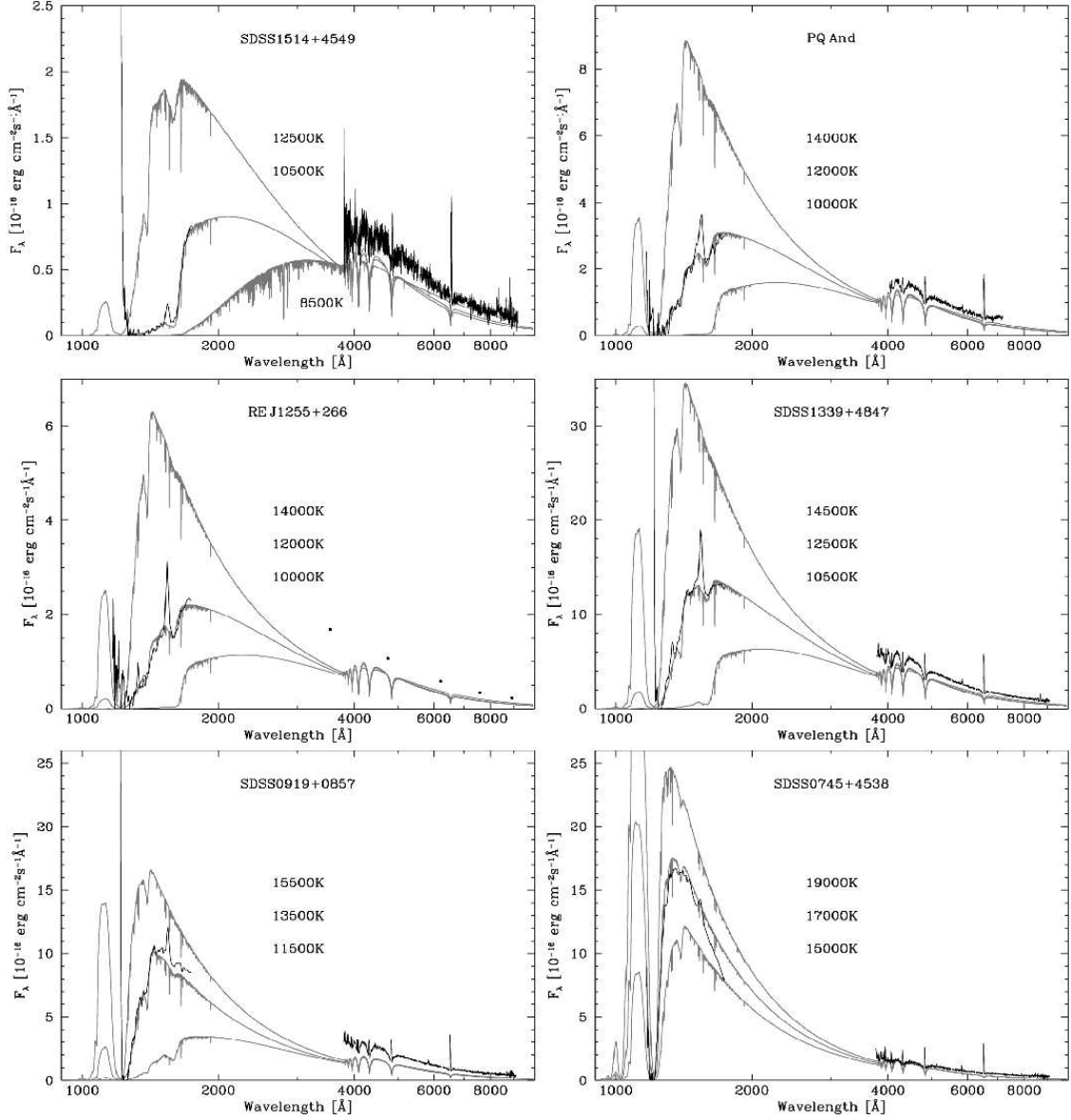


Fig. 4.— SBC data (with constant disk component removed) together with SDSS spectra (ugriz fluxes for REJ1255+26) for our 6 objects shown with dark lines. Grey lines are white dwarf models within 2000K of our best fit temperature white dwarfs. The difference between the WD model and the observed SDSS data is the disk contribution to the optical. Since SDSS0745+45 had an outburst since the SDSS spectra were obtained, the optical spectrum may not be representative of true quiescence.

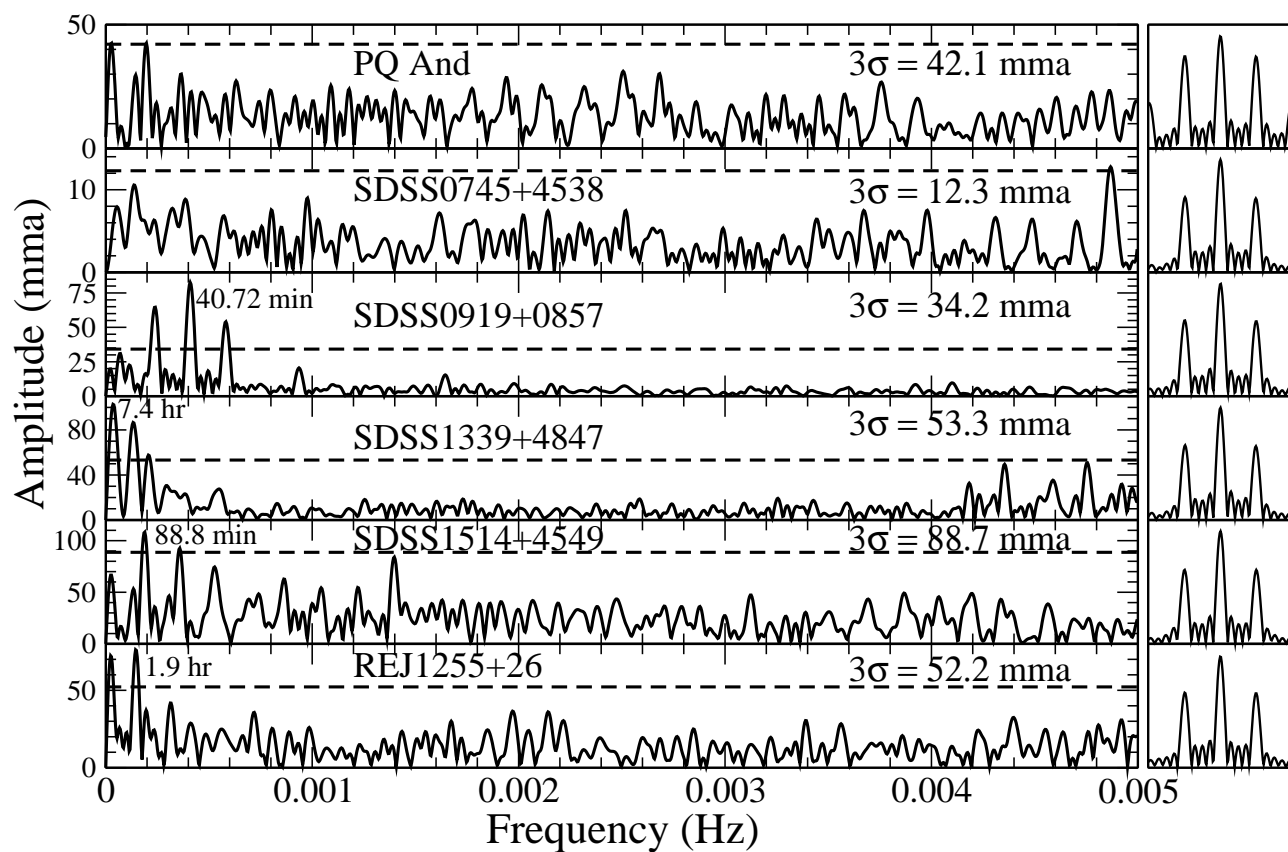


Fig. 5.— DFTs of the HST data for our 6 objects along with a dashed line showing the 3σ values of the noise for each object. The window functions are shown in the right-hand column, with the same scaling as the DFT along the x-axis.

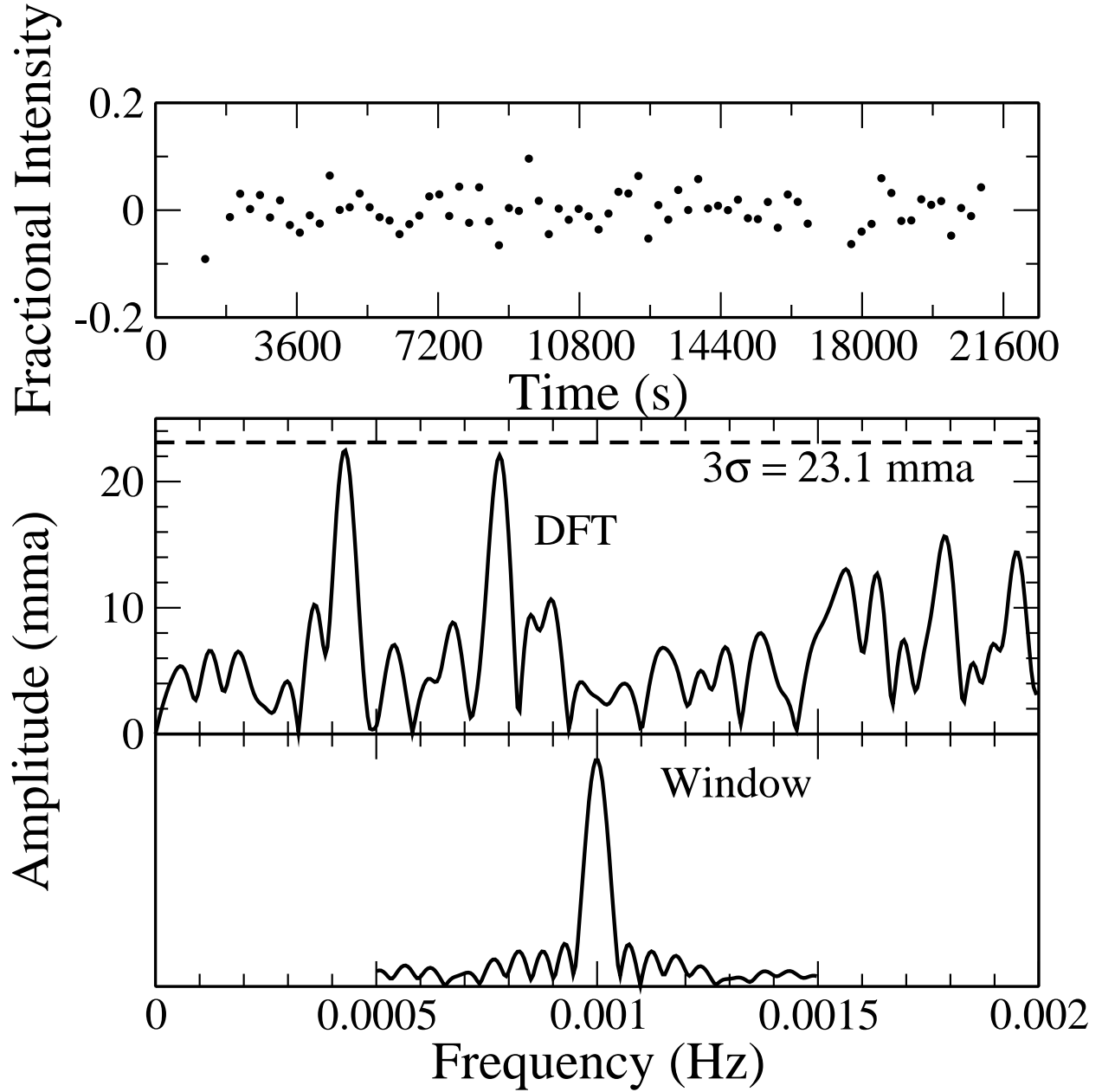


Fig. 6.— Normalized intensity (top), DFT (middle) and window function (bottom) of the NOFS data on PQ And taken simultaneously with the SBC on 2007 September 13. The two major peaks occur at 2337s and 1285s.

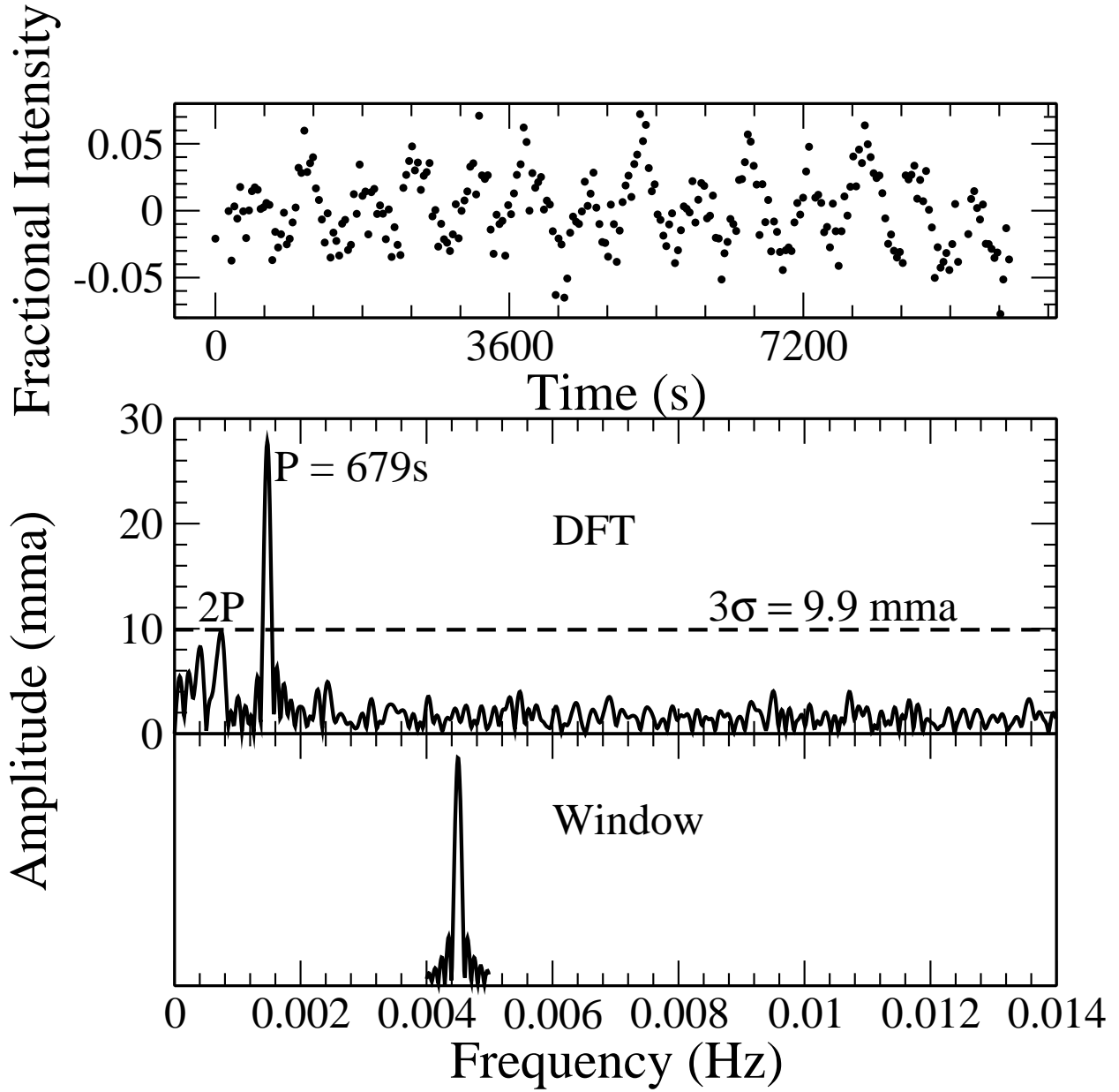


Fig. 7.— Intensity, DFT and window function for the WIYN data on PQ And obtained one year after the SBC data.

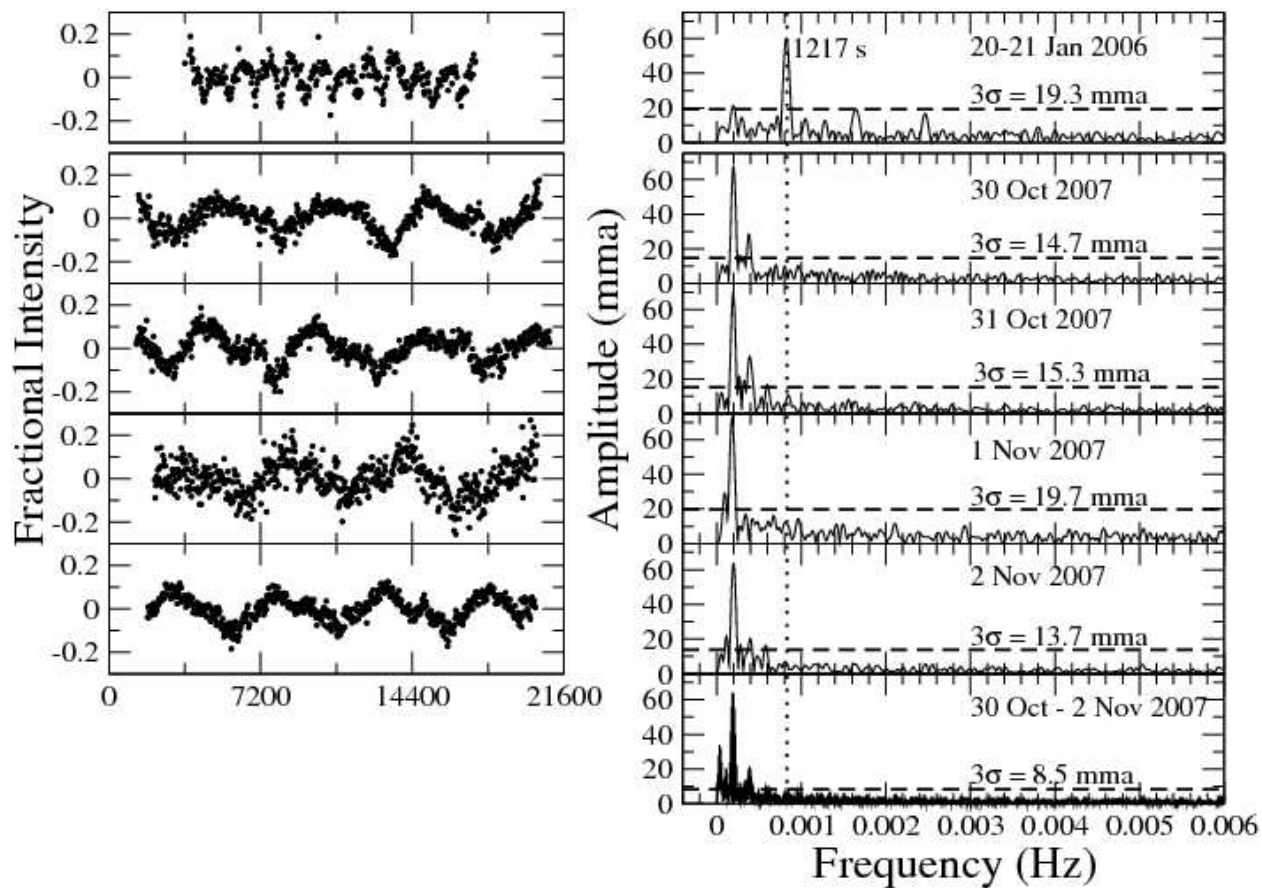


Fig. 8.— Comparison of SDSS0745+45 data from 2006 with the 4 nights surrounding the 2007 HST observations. Note the visible difference of the light curve as well as the changes in the period evident in the DFTs. Dashed lines show the 3σ values for the noise for each dataset.

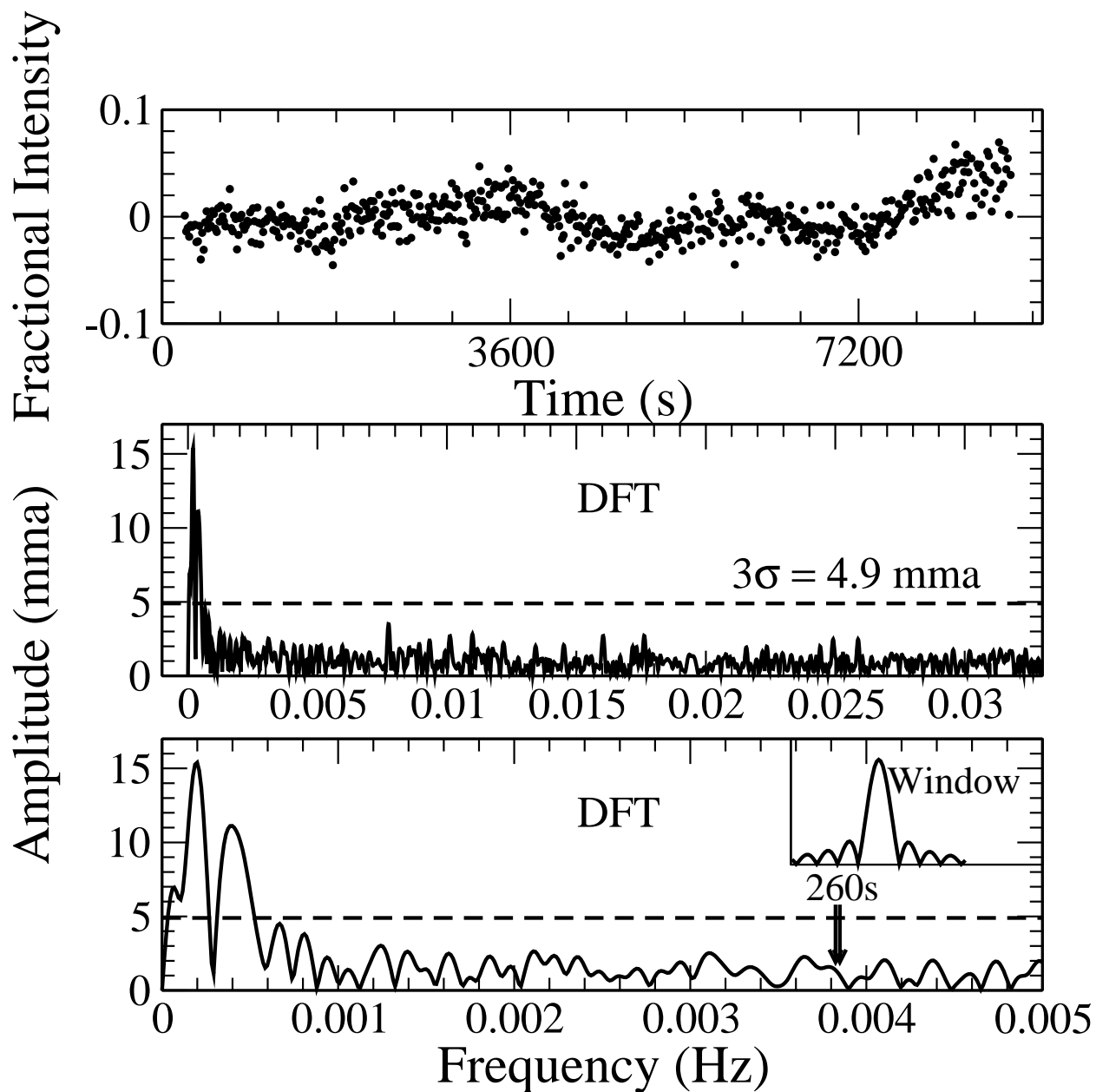


Fig. 9.— Intensity, DFT with window function, and expanded view of low frequencies for McDonald Observatory data on SDSS0919+08 obtained two nights prior to the HST data. The position of the 260s pulsation period that was previously observed is marked.

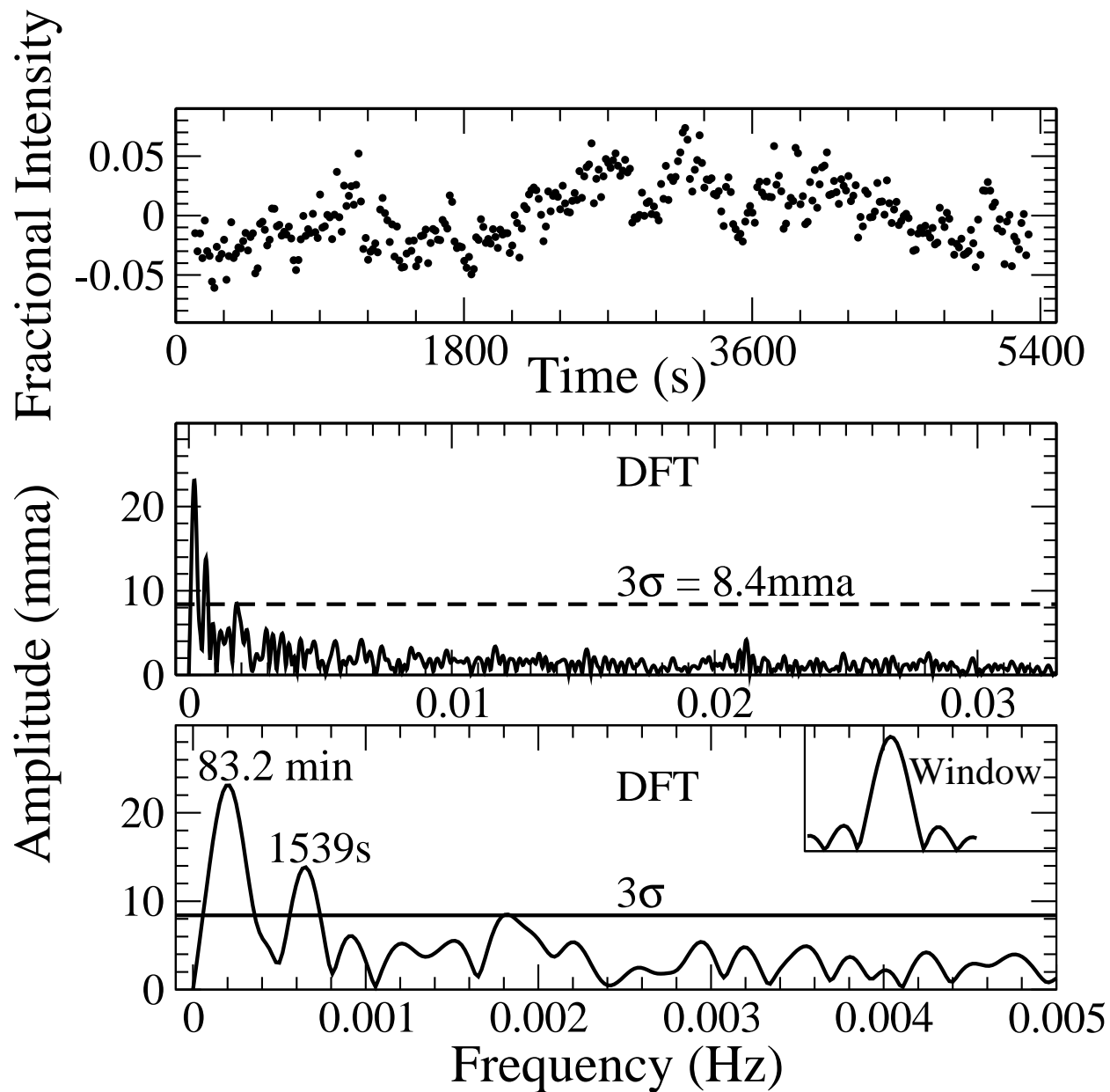


Fig. 10.— Intensity, DFT with noise level marked, and expanded view with window function for APO data on SDSS1339+48 obtained two nights prior to the HST data. The previously observed pulsation period at 641s (0.00156 Hz) is not evident.

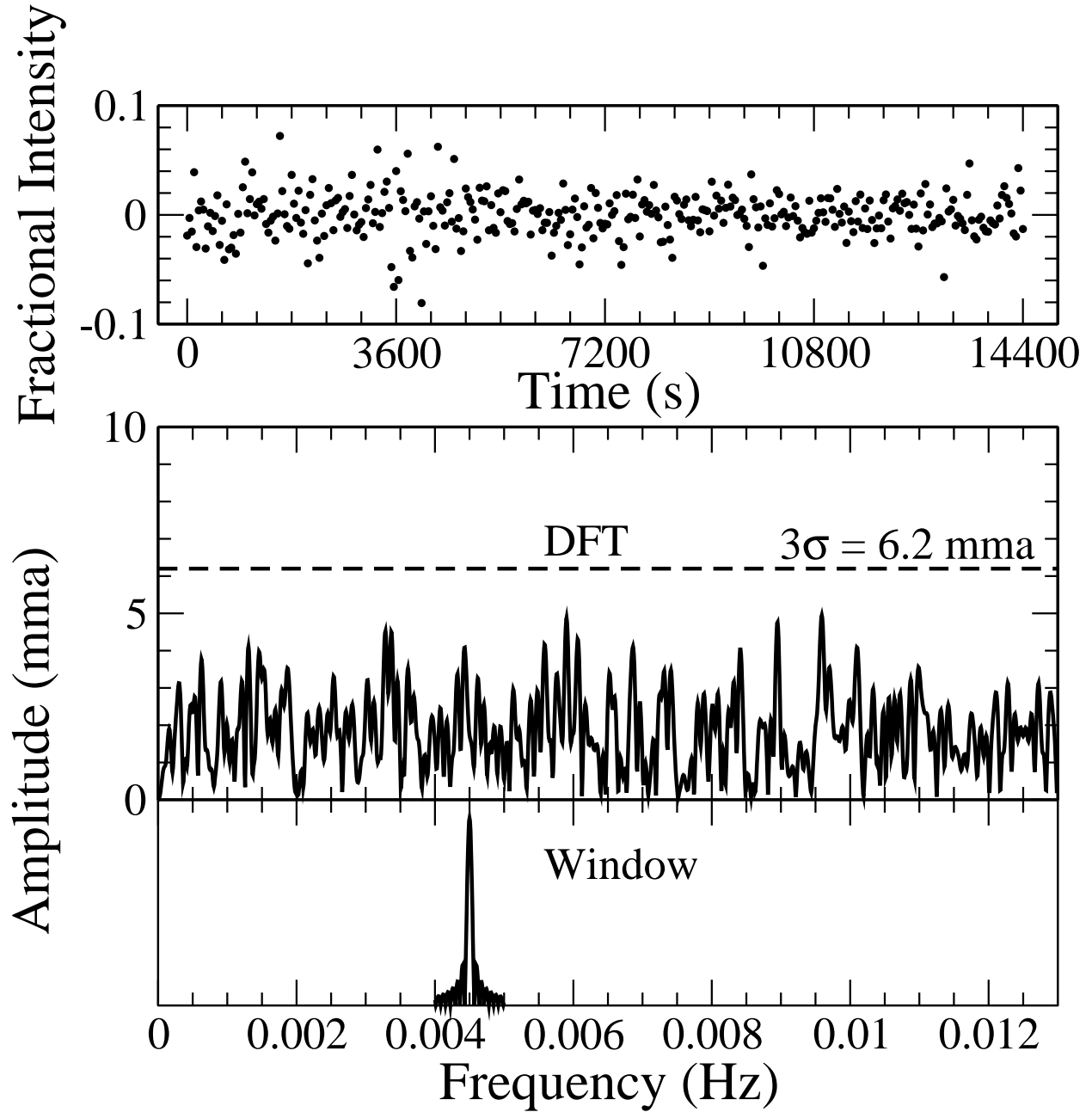


Fig. 11.— Intensity, DFT and window function for APO data on SDSS1514+45 that overlaps 1.5 hrs with HST observations. No periods are evident.

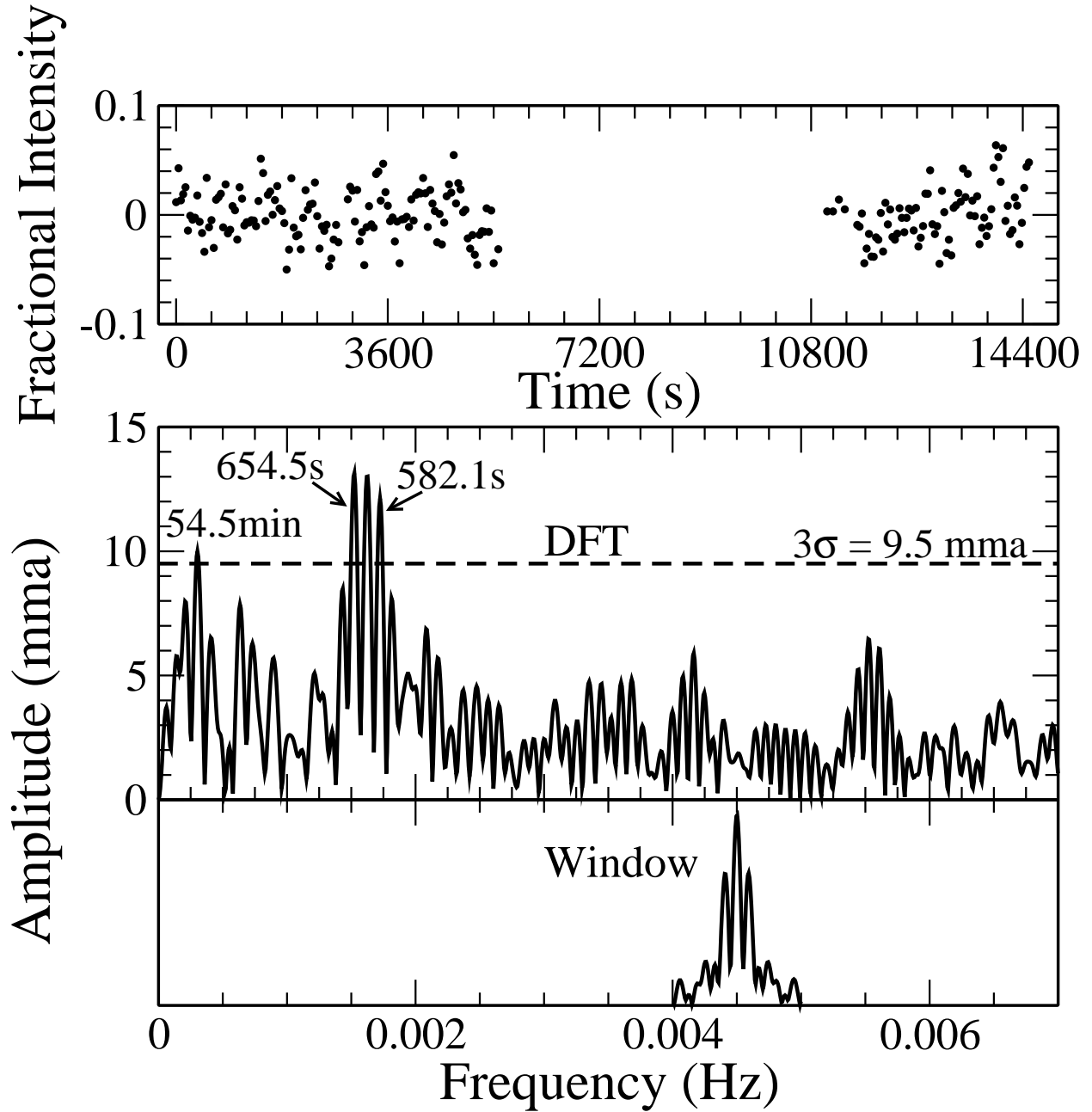


Fig. 12.— Intensity, DFT and window function for APO data on REJ1255+26 obtained one night after the HST data. Two significant short periods are evident.

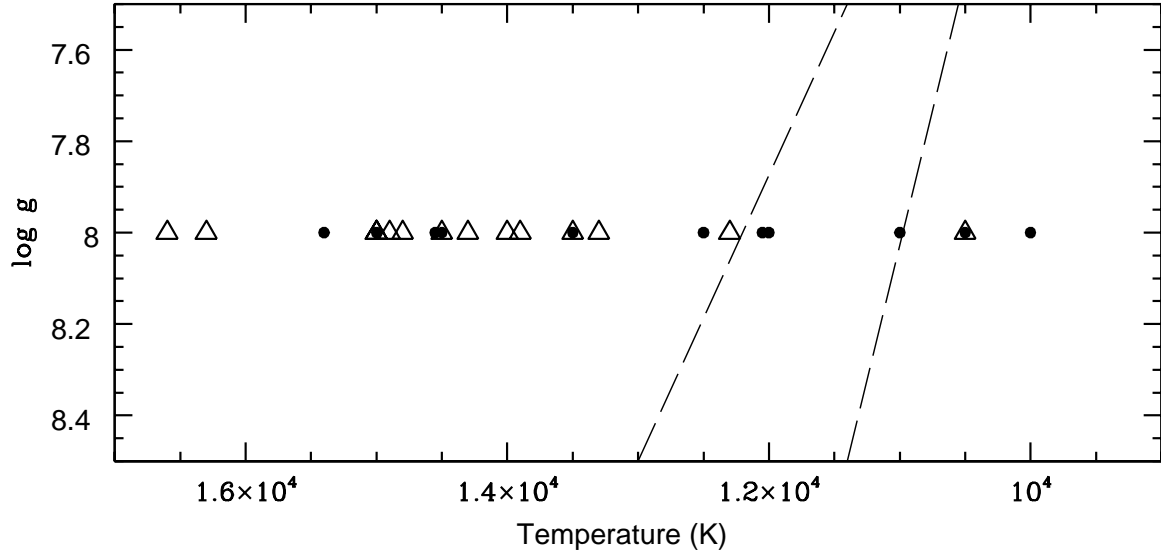


Fig. 13.— Temperatures of accreting pulsators (solid dots) and of non-pulsating CV white dwarfs (triangles) as a function of $\log g$. The ZZ Ceti instability strip limits (Gianninas et al. (2007)) are shown as dashed lines. The 3 pulsators within the strip are SDSS1507+52, REJ1255+26 and PQ And. The two objects just outside the blue edge are the non-pulsator EG Cnc and the pulsator SDSS1339+48.

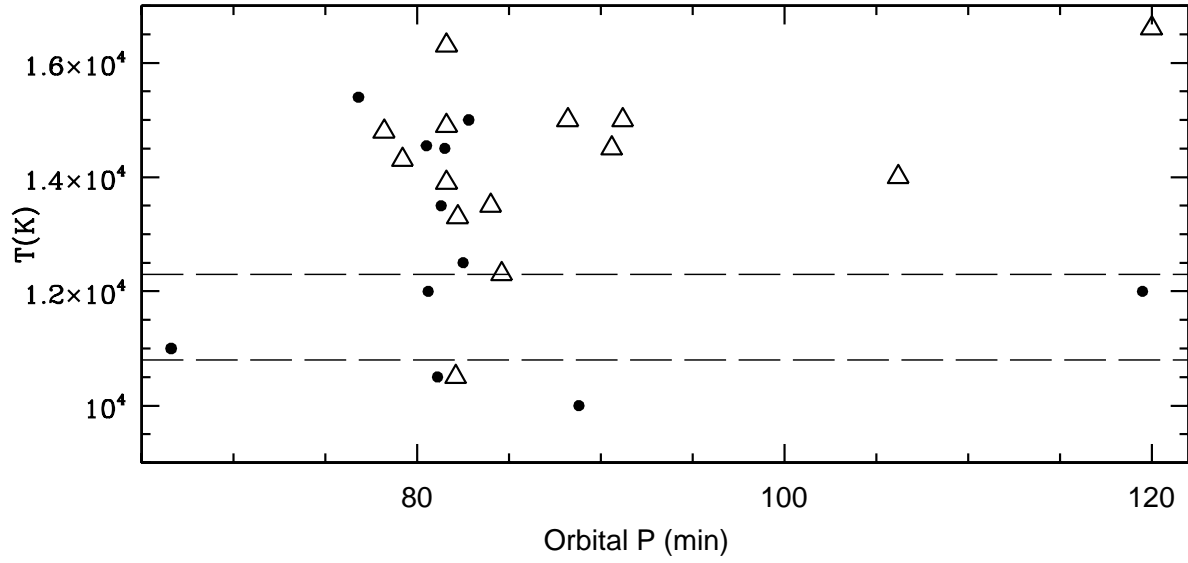


Fig. 14.— Temperatures of accreting pulsators (solid dots) and of non-pulsating CV white dwarfs (triangles) as a function of orbital period. The limits of the ZZ Ceti instability strip for $\log g=8$ (Gianninas et al. 2007) are shown as dashed lines.